

# Explosion-Induced Ignition and Combustion of Acetylene Clouds

Allen L. Kuhl

Lawrence Livermore National Laboratory  
Livermore, California, USA

Heinz Reichenbach

Ernst Mach Institut  
Freiburg im Briesgau, Deutschland

John B. Bell and Vincent E. Beckner  
Lawrence Berkeley National Laboratory  
Berkeley, California, USA

## 1 Introduction

In the past, we have studied combustion effects in both confined [1],[2] and unconfined explosions [3]. And we have proposed gasdynamic models of turbulent combustion in TNT explosions [4]. Here we investigate the explosion-induced ignition and combustion of acetylene clouds in a rectangular test chamber (Fig. 1). Chamber dimensions are: 101.5 mm x 101.5 mm x 386 mm. Gauges 1-5 were located on the centerline ( $y = 50.75$  mm) at  $x = 43, 118, 193, 268$  and  $343$  mm; gauges 6-10 were located near the side-wall ( $y = 20.75$  mm) at the same axial locations. A spherical PETN charge (mass between 0.2 and 0.5 grams with a density of 1 g/cc) was inserted into the chamber from the left wall on a wand. Charge axial locations varied from  $x = 75$  mm to 170 mm in different tests. The acetylene cloud was contained in a soap bubble film of various diameters (25, 40, 50 or 60 mm) typically located at  $x = 268$  mm.

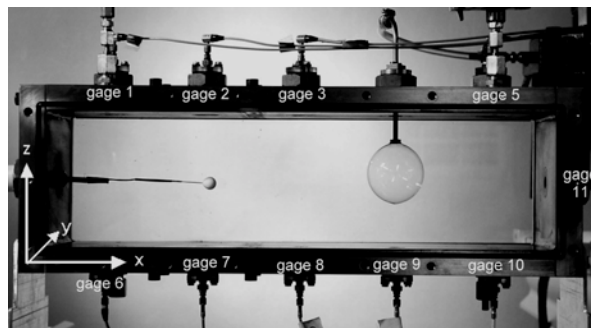


Figure 1. Photograph of the test chamber. In this test, a 0.5-g PETN-charge is placed at  $x = 96.5$  mm along the centerline ( $y = 50.75$  mm) of the chamber. The air-filled soap bubble ( $d = 50$  mm) is located at  $x = 268$  mm.

The charge was detonated by a high-voltage system described in [1]. This produced a blast wave that reflected from the walls, leading to complex Mach structures (Fig. 2:  $t = 152 \mu s$ ). The Mach fronts crush the soap bubble ( $t = 205 \mu s$ ) and deposit vorticity which causes turbulent mixing of the acetylene with air (Fig. 2:  $259 \mu s < t < 312 \mu s$ ).

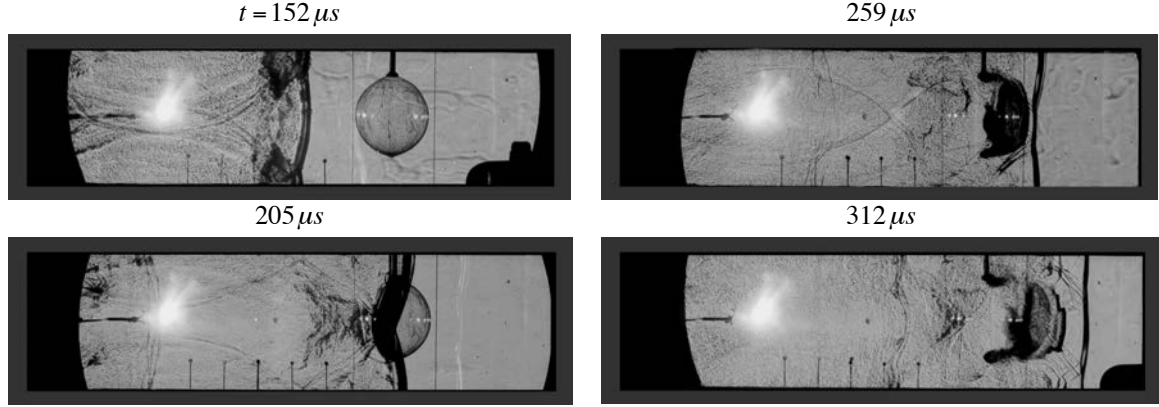


Figure 2. Schlieren photographs showing the evolution of a blast wave from a 0.3-g PETN charge, and its interaction with a 55-mm soap bubble filled with air.

## 2 Model

We model the system using the compressible Navier-Stokes equations for a reactive mixture [5], [6]. These equations express conservation of mass, momentum, total energy and species. If we assume unity Lewis number, so that species diffusion and thermal diffusion coefficients are the same, and ignore radiative effects, the system reduces to:

$$\partial_t \rho + \nabla \cdot (\rho U) = 0$$

$$\partial_t \rho U + \nabla \cdot (\rho U U) + \nabla p = \nabla \cdot \tau$$

$$\partial_t \rho E + \nabla \cdot (\rho U E + p U) = \nabla \cdot \kappa \nabla T + \nabla \cdot h_k \rho D_k \nabla Y_k + \nabla \cdot \tau U$$

$$\partial_t \rho Y_k + \nabla \cdot (\rho U Y_k) = \nabla \cdot (\rho D_k \nabla Y_k) + \dot{\omega}_k$$

where  $\rho$ ,  $U$ ,  $p$ ,  $T$  and  $Y_k$  are density, velocity, pressure, temperature and mass-fraction of species  $k$ , respectively. Here  $E = e + UU/2$  is the total energy and  $e = \sum_k e_k(T) Y_k$  is the internal energy. The stress tensor  $\tau = \mu(\nabla U + \nabla U^T) + \lambda \nabla \cdot U$  where  $\mu$  and  $\lambda$  are the viscosity coefficients and  $\kappa$  is the thermal conductivity. Lewis number of unity implies that the species mass diffusion  $\rho D_k = \kappa / c_p$ . For the simulations presented here we assume an ideal gas equation of state for the mixture:  $p = \rho RT \sum_k Y_k / W_k$  where  $W_k$  is the molecular weight of species  $k$ . The formulation specifies the thermodynamic behavior of the system using a Chemkin interface and includes the capability of model combustion as the ambient air mixes with the hydrocarbon cloud. Chemistry is modeled by a single-step reaction:  $C_2H_2 + 2.5O_2 \rightarrow 2CO_2 + H_2O$ :

$$\dot{\omega} = A e^{-E_a/RT} [C_2H_2]^{0.5} [O_2]^{2.5}$$

PETN products are  $H_2O$ ,  $CO_2$ ,  $CO$  and  $N_2$ .

The basic discretization uses a symmetric operator split formula in which we first advance the chemistry in each zone by  $\Delta t/2$ , then advance the Navier-Stokes equations without the reaction term by  $\Delta t$  and finally advance the chemistry by  $\Delta t/2$  again. The chemistry integration is performed using

standard techniques for ordinary differential equations. The integration algorithm for the Navier-Stokes equations combines an explicit, second-order, unsplit Godunov method for the hyperbolic part of the operator with a second-order, explicit Runge-Kutta algorithm for the diffusive terms.

The integration algorithm is embedded in a hierarchical adaptive mesh refinement algorithm. In this approach, fine grids are formed by dividing coarse cells by a refinement ratio  $r$ , in each direction. Increasingly finer grids are recursively embedded in coarse grids until the solution is adequately resolved with each level contained in the next coarser level. An error estimation procedure based on user-specified criteria where additional refinement is needed and grid generation procedures dynamically create or remove rectangular fine grid patches as resolution requirements change.

### 3 Results

The dynamics of the detonation products from a spherical 0.2-g PETN charge, and the ensuing ignition and combustion of a 50-mm acetylene bubble is depicted in Fig. 3. Cloud ignition occurs at  $t = 0.55 \mu\text{s}$ . It is this experiment that we have simulated with our compressible AMR code.

Figure 4 presents a three-dimensional volume rendering of the evolution of the temperature field of the acetylene cloud from the AMR simulation. It shows the flame dynamics in the turbulent combustion cloud. The first frame corresponds to the ignition of the cloud, which occurs at  $\sim 0.55 \text{ ms}$  in Fig. 3.

Figure 5 compares the pressure histories at gauge 5 for three cases: (1) 50 mm diameter C<sub>2</sub>H<sub>2</sub> bubble; (2) no bubble; and (3) AMR simulation. At early times (Fig. 5a), pressure histories in cases 1 and 2 are in close agreement, indicating that combustion has not influenced the flow (i.e., shock arrival times) at gauge 5 over that time domain. The AMR pressure record is in qualitative agreement with the data records. At later times (Fig. 5b), the pressure record from case 2 diverges from case 1; by 8 ms combustion has increased the pressure to  $\sim 3.3$  bars (versus 1.5 bars for the no bubble case)—thereby illustrating the effect of energy release due to combustion in confined explosions. Beyond 8 ms, radiative losses begin to cool the fireball, thereby causing a gradual pressure decay. The pressure history from the AMR simulation is in qualitative agreement with measured pressure history for case 1 out to 8 ms, however the frequency content is somewhat lower in the simulation.

### 4 Summary

The proposed AMR code model—based on the compressible Navier-Stokes equations for a reactive mixture—is able to capture the major features of ignition and evolution of turbulent combustion cloud in this problem. It would be interesting to study other experiments in this test series (different bubble diameters, different charge-bubble separations, etc.) to establish the limits of this modeling approach.

### References

- [1] Kuhl, AL, Reichenbach, H. (2009). Combustion effects in confined explosions, *Proc. Combustion Institute* **32** (2) pp. 2291-2298.
- [2] Kuhl, AL, Reichenbach, H (2010). Barometric calorimeters, *Comb., Exp. & Shock Waves*, **4** (2) pp. 271-278.
- [3] Kuhl, AL, Bell, JB, Beckner, VE, Balakrishnan, K, Aspden, AJ. (2013). Spherical combustion clouds in explosions, *Shock Waves* **23** (3), pp. 233-249.
- [4] Kuhl, AL, Bell, JB, Beckner, VE, Reichenbach, H. (2011). Gasdynamic model of turbulent combustion in TNT explosions, *Proc. Combustion Institute* **33** pp. 2117-2185.
- [5] Bell, JB, Day, MS. (2011). Chapter 13: Adaptive methods for simulation of turbulent combustion, *Turbulent Combustion Modeling*, Echekki and Mastourakos (eds.), Fluid Mechanics and Its Applications **95**, Springer Science+Buisenss Media B, pp. 301-329.
- [6] Bell, JB. (2012). AMR for low Mach number reacting flow, *Proc. Chicago Workshop on Adaptive Mesh Refinement Methods*, pp. 203-221.

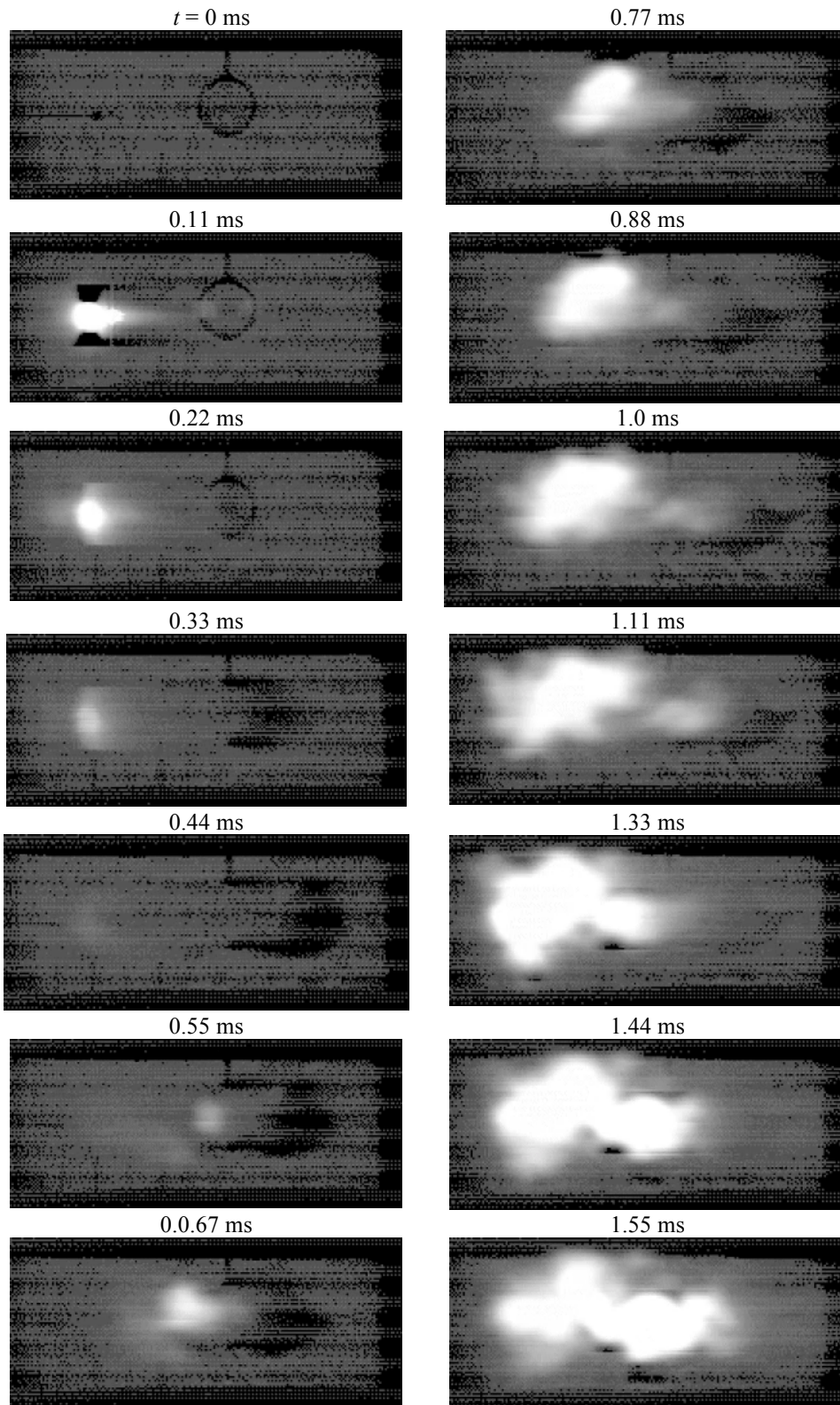


Figure 3. Video photography of the dynamics of the detonation products from a spherical 0.2-g PETN charge at  $x = 130$  mm, and the ignition/combustion of a 50-mm acetylene bubble located at  $x = 170$  mm (Test #72); Framing rate = 9 kHz.  $t_i \sim 0.55$  ms.

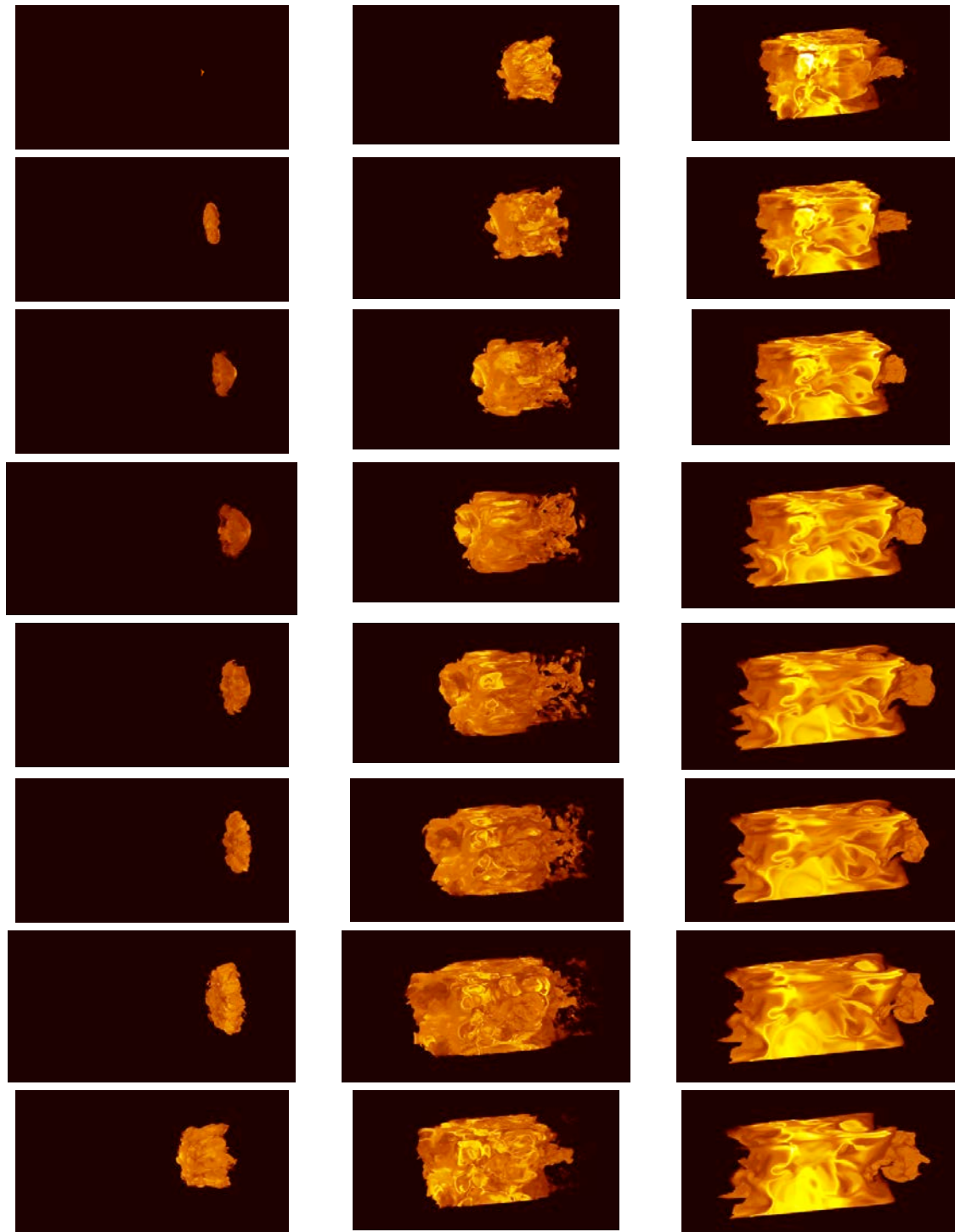


Figure 4. Three-dimensional volume rendering of the temperature field of the acetylene cloud is used to visualize the flame dynamics in the turbulent combustion field from the AMR simulation (frame rate = 10 cycles). Temperature field of the PETN detonation products cloud has been removed in order to focus on acetylene combustion dynamics.

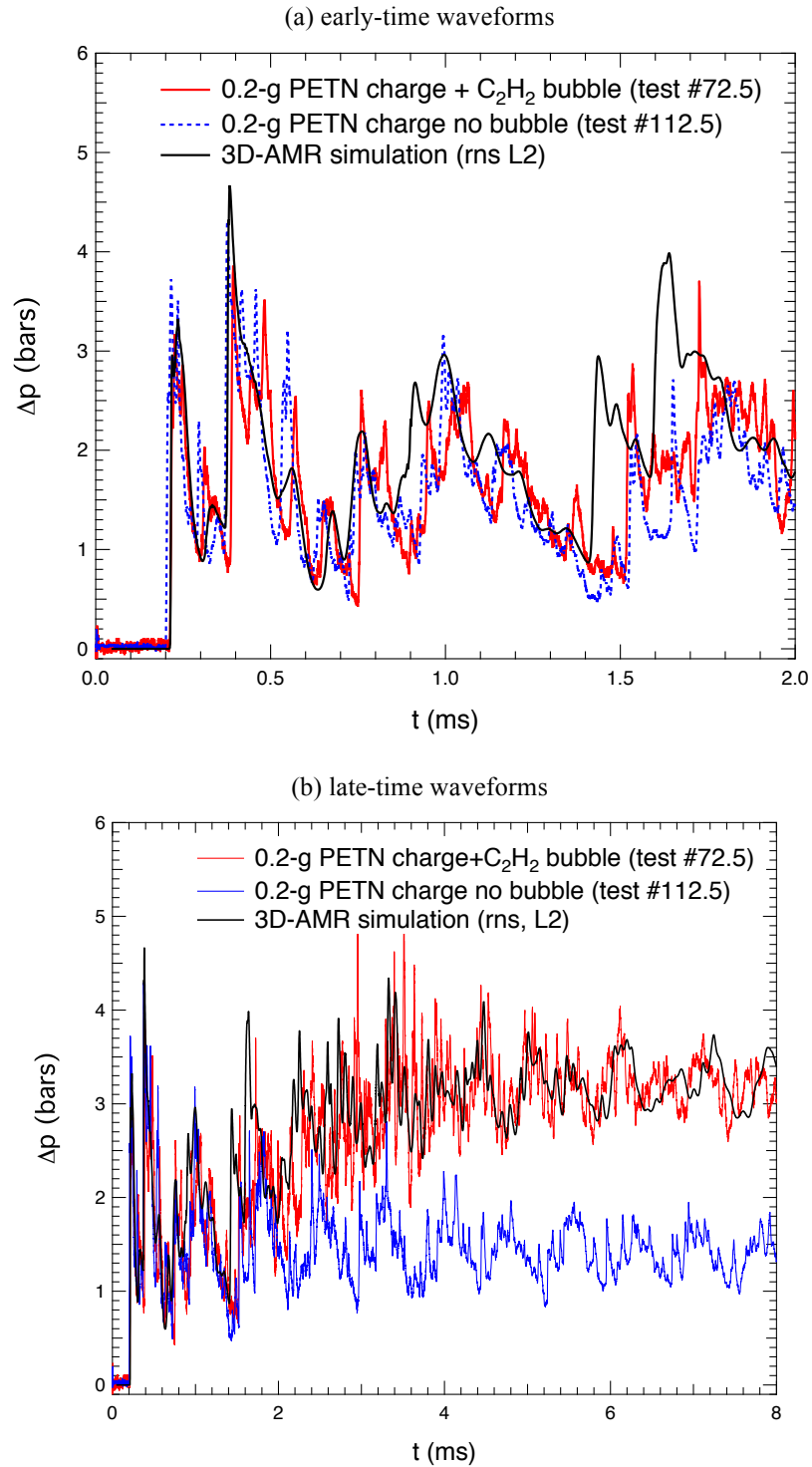


Figure 5. Pressure histories at gauge 5 for a 0.2-g spherical PETN charge detonated in the tunnel filled with air. Case 1: with an acetylene bubble ( $d = 50$  mm), Case 2: no bubble; Case 3: 3D-AMR code simulation.

**COMMENT:** The frequency content in the numerical simulation depends on the grid resolution; it takes 2-3 cells for a discontinuity to reach its post shock state. The frequency content in the pressure records depend on the gauge diaphragm “effective diameter” ( $\sim 3$  mm), its natural frequency (measured at  $\sim 400$  kHz) and data digitization rate (1 MHz). The numerical simulation captures the major wave features; to capture the fine-scale structure one would need considerably finer grids (which is beyond the scope of the present study).